Research paper

New bands of deuterated nitrous acid (DONO) in the near-infrared using FT-IBBCEAS

Ranjini Raghunandan[a,1], Johannes Orphal[b], Albert A. Ruth[a,*]

[a] Physics Department and Environmental Research Institute, University College Cork, Cork, Ireland
[b] Institute of Meteorology and Climate Research, Karlsruhe Institute of Technology, Hermann-von-Helmholtz-Platz 1, 76344 Eggenstein-Leopoldshafen, Germany

HIGHLIGHTS

- Simultaneous detection of multiple isotopologues with FT-IBBCEAS in the near-IR.
- Experimental/spectroscopic characterization of combination and overtone bands of DONO.
- Experimental detection and confident assignment of two new DNO_3 bands.

ARTICLE INFO

ABSTRACT

The first measurements of near-infrared bands of deuterated nitrous acid (DONO) are presented. The measurements were made using Fourier-Transform Incoherent Broad-Band Cavity-Enhanced Absorption Spectroscopy (FT-IBBCEAS) in the 5800–7800 cm^{-1} region. Two bands of *trans*-DONO centred at 6212.029 and 7692.496 cm^{-1} were observed and assigned to the $2\nu_1 + \nu_3$ combination and $3\nu_1$ overtone vibrations, respectively. Their rotational band structure was satisfactorily reproduced using PGOPHER. For *cis*-DONO the $3\nu_1$ band was observed at ~7302.5 cm^{-1}. In addition, new bands centred at 6142.5 cm^{-1} and 7607.6 cm^{-1} were quite confidently assigned to the $2\nu_1 + \nu_3$ and $3\nu_1$ vibrations of deuterated nitric acid, DNO_3, respectively.

1. Introduction

Nitrous acid, HONO, has been the subject of numerous spectroscopic studies [1–12]. One of the main reasons for studying this species and in its deuterated counterpart DONO [13,14] is its important role in atmospheric photochemistry. As the main precursor of the hydroxyl (OH) radical in polluted urban areas [15,16], HONO plays a significant role in the formation of ozone in the troposphere. The hydrolysis of NO_2 on heterogeneous surfaces is the proposed mechanism for formation of nitrous acid, resulting also in HNO_3 as by-product [17–19]. Atmospheric and laboratory measurements of HONO are essential to understand its molecular and photochemical properties as well as the processes of its formation. The near-infrared region is interesting in these aspects because it might play a role in photodissociation from vibrationally excited ("solar pumped") states [20], and also because it is well suited for fast HONO detection in chemical reactions [21].

HONO and DONO are planar molecules with C_s symmetry, having six vibrational fundamental modes and two isomeric forms [22,23]. The

trans-isomer is the thermodynamically preferred configuration in both cases, as determined by measurements in the microwave region [24]. The energy difference between the ground vibrational states of *trans*- and *cis*-HONO was re-investigated by *Sironneau et al.* [25] by considering the relative absorption line intensities in the far infrared, which were used to determine the zero-point and ground state energy differences of *trans*- and *cis*-HONO and -DONO. The zero-point corrected ground state energies of the *cis*-isomers of HONO and DONO lie ~107 cm^{-1} and ~114 cm^{-1} above that of the corresponding *trans*-form [23]. Therefore the ground states of the *cis*-isomers of both isotopologues are thermally populated at room temperature (296 K) at somewhat less than 60% of that of the *trans*-form.

In contrast to HONO, there have been much fewer studies on DONO [12–14]. In fact, no absorption band of DONO has been measured up-to-date in the near-infrared region. High-resolution Fourier-transform spectra of DONO were first recorded by *Halonen et al.* [13], who analysed the ν_3, ν_4, ν_5 and ν_6 fundamental bands of *trans*-DONO and the ν_4 fundamental of *cis*-DONO. The ν_3 band of *trans*-DONO was observed to

---

be perturbed by the nearby $\nu_5 + \nu_6$ vibrational state [13]. The ground state constants published in this work were later revised by *Dehayem-Kamadjeu et al.* [12] using pure rotational spectra in the far-infrared region between 40 and 150 cm^{-1}. Detailed studies of the ν_1 fundamental band of *trans-* and *cis-*DONO between 2350 and 3000 cm^{-1} measured at 0.003 cm^{-1} resolution, were also carried out by the same group [14]. Unlike the ν_1 band of HONO, no strong perturbations were observed for either isomer of DONO. The *trans-*isomer showed very small perturbation for the Q-branch, shifting some lines by up to 0.01 cm^{-1}, while the ν_1 band of *cis-*DONO showed no rotational perturbation at all. This was attributed to the distribution of vibrational energy levels, supported by coupled-cluster ab-initio calculations [26], which predict the nearest states to ν_1 to be at least 50 cm^{-1} away in energy.

In this work, we report measurements of the $2\nu_1 + \nu_3$ and the $3\nu_1$ bands of *trans-*DONO and the $3\nu_1$ band of *cis-*DONO in the near-infrared region using Fourier-Transform Incoherent Broad-Band Cavity-Enhanced Absorption Spectroscopy (FT-IBBCEAS) [27–29]. All bands were sufficiently resolved to yield spectroscopic constants with reasonable accuracy. In addition, the first observation of the $2\nu_1 + \nu_4$ and the $3\nu_1$ (O-D stretch) bands of deuterated nitric acid (DNO$_3$) is reported. Several bands of HONO, HNO$_3$ and NO$_2$ have been detected simultaneously over the full spectral measurement range (5800–7800 cm^{-1}), demonstrating the potential of this method to detect different species which might be of interest for future laboratory studies of nitrogen oxides and their related acids.

2. Experimental

All spectra were recorded at a resolution of 0.08 cm^{-1} between 5800 and 7800 cm^{-1} using FT-IBBCEAS [27,28]. IBBCEAS measures the intensity of light transmitted by a stable optical cavity consisting of high reflectivity mirrors (typically $R > 99.9\%$) [29]. The transmission signal strength is measured with and without the absorber of interest present inside the cavity ($I(\lambda)$ and $I_0(\lambda)$ respectively). From the ratio of the wavelength-dependent transmitted intensities, the reflectivity of the mirrors $R(\lambda)$, and the sample path length per pass d inside the cavity, the sample's extinction coefficient $\varepsilon(\lambda)$ is calculated as $\varepsilon(\lambda) \approx \frac{1}{d}\left(\frac{I_0(\lambda)}{I(\lambda)} - 1\right)(1 - R(\lambda))$. Broadband spectroscopy allows a significant spectral range to be covered simultaneously. This multiplex advantage enables several species to be monitored at once, while
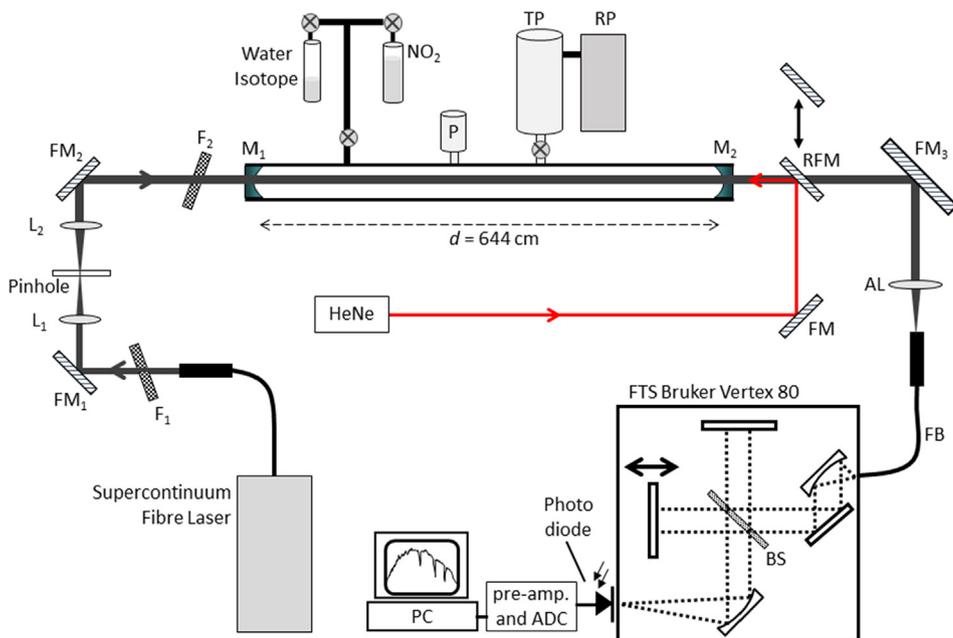
gathering information over the entire spectral region [30].

A schematic sketch of the experimental setup is shown in Fig. 1 (also see Ref. [31]). The FT-IBBCEAS set-up employs a supercontinuum fibre laser (Fianium, SC450, ~5 W) which has a spectral output from about 5500 to 20000 cm^{-1}. It runs at a repetition rate of 60 MHz delivering pulses of about 5 ps duration. The optical cavity of 644 cm physical length consisted of two high reflectivity mirrors ($R \sim 0.999$ from ~5714 to 8000 cm^{-1}, diameter 40 mm, Layertec GmbH). For measurements in the region of interest, a long-pass filter with cut-on wavelength at ~9090 cm^{-1} (Thorlabs, FEL1100nm) was introduced between the laser and the cavity to avoid too much optical power reaching the detector outside the high reflectivity range of the mirrors. The light exiting the cavity was coupled into a Fourier-transform spectrometer (Bruker, Vertex 80), and the transmitted intensity after the cavity was typically integrated for 10 min by averaging over 20 individual interferograms, which were stablished through continuous scanning. The mirror reflectivity was determined by filling the chamber with a known concentration of CO$_2$ (pressure 6 mbar), and estimating the extinction coefficient based on the absorption cross-section of the sample at the wavenumbers where CO$_2$ absorption lines are available. From our measurements, we estimate the reflectivity to be 0.9986 at ~6050 cm^{-1}, where the $2\nu_3 + \nu_1$ band of *trans-*DONO is located; this corresponds to an effective pathlength of ~4.6 km in that wavenumber region.

3. Results and discussion

As a first test of the FT-IBBCEAS set-up, simultaneous measurements of HONO, HNO$_3$ and NO$_2$ were carried out by introducing 3.6 mbar NO$_2$ into the cavity. The NO$_2$ reacted with the residual water vapour on the cavity walls, forming HONO and HNO$_3$. An overview spectrum across a broad spectral range spanning > 2000 cm^{-1} was measured, from which simultaneous information on several bands of HONO, NO$_2$ and HNO$_3$ was obtained. Fig. 2 presents a portion of the FT-IBBCEAS spectrum which was obtained using an acquisition time of 5 min at a resolution of 0.08 cm^{-1}. For NO$_2$ the *lower limit* of the absorption cross section was estimated for the strongest line in the $\nu_1 + 3\nu_3$ band at ~5994.4 cm^{-1}. A value of ~3.1 × 10^{-22} cm^2/molecule was derived from the calibrated reflectivity in that region and the initial pressure of NO$_2$. Since NO$_2$ losses occur in the generation of HONO and HNO$_3$, the above value is merely a lower limit.

Fig. 1. Schematic of the FT-IBBCEAS setup: (R) FM: (removable) flat mirror; FB: fibre bundle; (A)L: (achromatic) anti-reflection coated infrared lenses; BS: beam splitter; F$_1$: notch filter (9400 cm^{-1}), tilted; F$_2$: long-pass filter, tilted; M: highly reflective spherical (cavity) mirror; HeNe: alignment laser; P: pressure gauge; RP: rotary pump (10^{-2} mbar); TP: turbo-molecular pump (10^{-5} mbar). Photodiode: InGaAs (~1 mm^2 area, at room temperature).
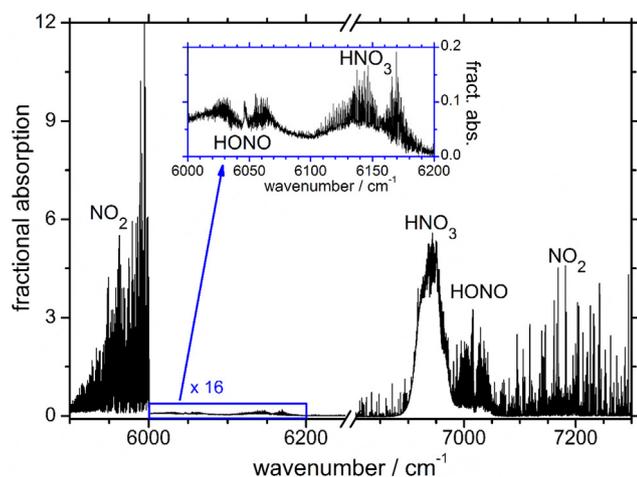
Fig. 2. Fractional absorption (I_0/I-1) spectrum of a mixture of NO_2, HONO, HNO_3 and H_2O in the near-infrared measured by FT-IBBCEAS. The spectral resolution is 0.08 cm^{-1}. The strong band around 7010 cm^{-1} is assigned to the $2\nu_1$ band of the *trans*-HONO species, and the strong band around 6950 cm^{-1} to the $2\nu_1$ band of HNO_3. The NO_2 bands below 6000 cm^{-1} and around 7190 cm^{-1} are the $\nu_1 + 3\nu_3$ and $2\nu_1 + 3\nu_3$ bands, respectively [32].

Fig. 4. Measured (black) and modelled (red) $2\nu_1 + \nu_3$ combination band of *trans*-DONO. See Table 1 for the upper state's rotational constants. A temperature of 300 K was used for the simulation. The Q-branch in the modelled spectrum is sharper, probably due to differences in the centrifugal distortion constants, and possibly also line-mixing. (For interpretation of the references to colour in this figure legend, the reader is referred to the web version of this article.)
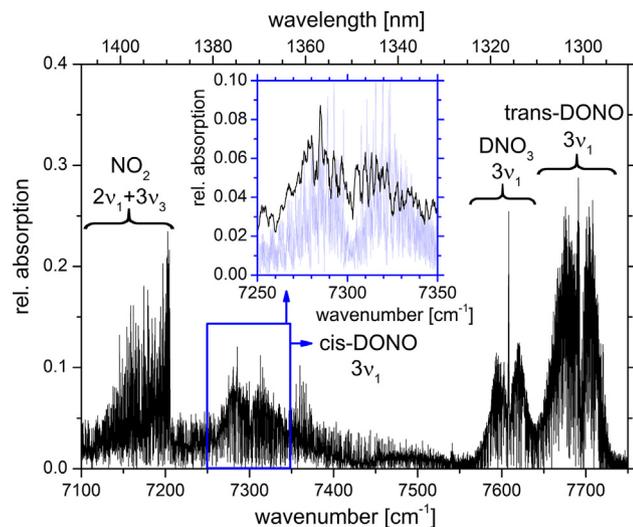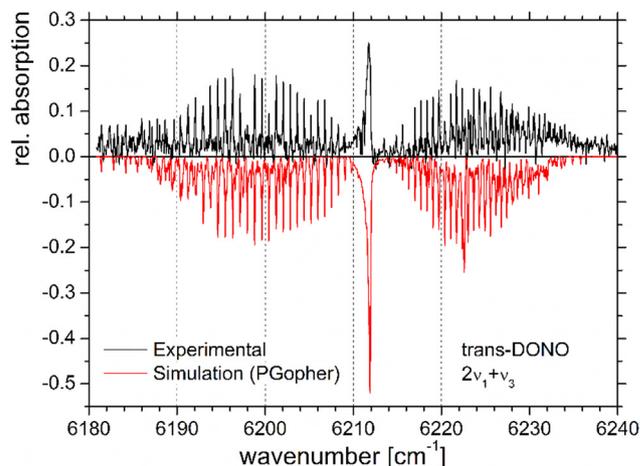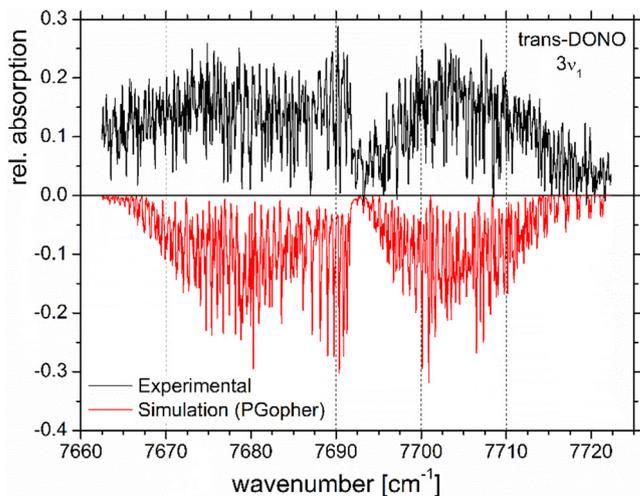

Fig. 3. Overview spectrum of deuterated species following the passivation of the measurement cell with D_2O and subsequent filling with NO_2. Inset: $3\nu_1$ band of *cis*-DONO; observed (black) and simulated (light blue trace). Both traces were smoothed by adjacent averaging (100 pts). The similarity of the band shapes in the inset indeed corroborates this band being the $3\nu_1$ overtone of *cis*-DONO. (For interpretation of the references to colour in this figure legend, the reader is referred to the web version of this article.)

Fig. 5. Measured (black) and modelled (red) $3\nu_1$ overtone band of *trans*-DONO. The agreement is quite satisfactory despite some noise in the measured spectrum. See Table 1 for the upper state's rotational constants. A temperature of 300 K was used. Note the K-structure of the Q-branch in both the measured and the modelled spectrum. (For interpretation of the references to colour in this figure legend, the reader is referred to the web version of this article.)

To produce a sample of DONO, the cavity was first passivated overnight with D_2O, following measurements of a mixture of 6.5 mbar of D_2O and 4 mbar of NO_2. The reaction of NO_2 with D_2O produced *trans*- as well as *cis*-DONO. Also overtone bands of DNO_3 were detected for the first time as a result of its formation as by-product of the reaction between NO_2 and D_2O. The FT-IBBCEAS measurements showed one new vibrational overtone of *cis*-DONO and two new vibrational overtone bands of *trans*-DONO (Figs. 3–5). In Fig. 3 the spectral region from 7100 to 7750 cm^{-1} of the deuterated species is shown, which contains the $3\nu_1$ bands of *cis*- and *trans*-DONO.

3.1. Cis-DONO

To corroborate the assignment of the band at 7302 cm^{-1} a line-by-line simulation with the same software as used in Ref. [14] was

performed and compared with the measured spectrum, shown in the inset of Fig. 3. For the simulation, the rotational and centrifugal distortion constants of the ν_1 band of *cis*-DONO from *Dehayem et al.* [14] were used and then extrapolated to estimate those of the $3\nu_1$ overtone state. The calculation used an S-reduced Watson Hamiltonian in the I^r representation [33]. As observed for the ν_1 band [14], a pure *b*-type spectrum was assumed for the $3\nu_1$ band. Only the band centre was adjusted to achieve good overall agreement. The similarity of the band shapes in the inset of Fig. 3 indicates that this band is indeed the $3\nu_1$ band of *cis*-DONO.

3.2. Trans-DONO

Trans-DONO is a near-prolate asymmetric top (κ = -0.95). For the analysis of the rotational structure of the $2\nu_1 + \nu_3$ and $3\nu_1$ vibrational bands of *trans*-DONO (shown in Figs. 4 and 5), it was assumed that the

Table 1

Spectroscopic constants (in cm^{-1}) of the $2\nu_1 + \nu_3$ and $3\nu_1$ bands of *trans*-DONO and of the $3\nu_1$ band of *cis*-DONO. The S-reduced Watson-Hamiltonian in the I^r representation was used [33]. (a) Values obtained in this study from a fit using PGOPHER [34]. Numbers in parentheses are 1σ uncertainties in units of the last digit. (b) Values from *Dehayem et al.* (2006) [14]. (c) Vibrational dependence of rotational and centrifugal distortion constants from Ref. [14] extrapolated to three quanta of ν_1, only the band centre was adjusted to match the simulated with the observed data.

Constants	*trans*-DONO		*cis*-DONO		
	$2\nu_1 + \nu_3$ [a]	$3\nu_1$ [a]	Ground state [b]	ν_1 [b]	$3\nu_1$ [c]
[cm^{-1}]					
ν_0	6212.0292(55)	7691.7816(80)	0	2533.57024	7302.5(10)
A	2.97701(33)	2.92322(35)	2.362141725	2.3468943	2.31639945
B	0.396052(39)	0.379061(63)	0.430266983	0.43153178	0.43406137
C	0.330203(39)	0.355008(58)	0.363294673	0.36382322	0.36488032
D_K	$5.16(61) \times 10^{-5}$	$8.57(30) \times 10^{-5}$	34.31537	33.5602	32.04986
D_{JK}	$-5.4(60) \times 10^{-7}$	$-3.37(55) \times 10^{-6}$	0.066188	0.05882	0.044084
D_J	$3.90(43) \times 10^{-7}$	$-7.83(53) \times 10^{-7}$	0.5464628	0.544592	0.5408504

excited vibrational state has A$_1$ symmetry. The rotational structure of the upper levels was then modelled with the PGOPHER software [33] using the known ground-state rotational and centrifugal distortion constants [12], which were kept constant in the analysis. A Gaussian linewidth of 0.10 cm^{-1} and a rotational temperature of 300 K were used for the spectral modelling.

The band centres of $2\nu_1 + \nu_3$ and $3\nu_1$ were determined to be at 6212.0292 and 7692.4960 cm^{-1}. The central *Q*-branches are the most dominant features. No resolved line structure is observed for the $2\nu_1 + \nu_3$ combination band (see Fig. 4), but a beautiful *K*-substructure is observed for the $3\nu_1$ overtone band (see Fig. 5). Both bands show distinct *a*-type features in the *P*- and *R*-branches with spacings of about 0.7 cm^{-1} (about B + C, characteristic for parallel bands of prolate symmetric tops). One can assign *a*-type ^qQ_K lines up to K$_a$ = 12 in the case of *trans*-$3\nu_1$ (see Fig. 5).

The spectroscopic constants from the PGOPHER analysis of the *trans*-DONO bands are summarized in Table 1 together with the constants used for modelling the *cis*-DONO band in the inset of Fig. 3. All quantities in the S-reduced Watson-Hamiltonian (I^r representation) that are not shown in the table were fixed to zero in the calculation. This is justified by the much smaller values of d$_1$ and d$_2$ for DONO compared to the diagonal centrifugal distortion constants [14].

In Table 2 some known elements of the harmonic progression of the ν_1 vibration are compared for both isomers of HONO and DONO. As expected the anharmonicity of the $3\nu_1$ for DONO is smaller than that of HONO based on the larger mass of DONO [35]. *cis*-DONO appears to be somewhat more anharmonic than *trans*-DONO (by ~38 cm^{-1}), which follows the same trend as for the $2\nu_1$ of *cis*-HONO and *trans*-HONO, where again *cis*-HONO shows the larger anharmonicity (~24 cm^{-1}); see Table 2.

3.3. DNO$_3$

In the NO$_2$/H$_2$O mixture, in addition to nitrous acid HONO, nitric acid, HNO$_3$, was observed (see Fig. 2) in the FT-IBBCEA spectrum. Similarly, the FT-IBBCEA spectrum of a NO$_2$/D$_2$O mixture, apart from the

Table 2

Energies (in cm^{-1}) of the fundamental, first, and second overtones of the ν_1 vibrational mode in *trans*- and *cis*-HONO and -DONO. (a) Values from *Mélen and Herman* [36]. (b) Values from *Dehayem et al.* [14]. (c) Values obtained in this study.

	ν_1 [cm^{-1}]	$2\nu_1$ [cm^{-1}]	anharmonicity [cm^{-1}]	$3\nu_1$ [cm^{-1}]	anharmonicity [cm^{-1}]
trans-HONO	3590[a]	7017[a]	−163[a]	10,280[a]	−490[a]
trans-DONO	2651[b]			**7692**[c]	**−261**[c]
cis-HONO	3426[a]	6665[a]	−187[a]		
cis-DONO	2534[b]			**7303**[c]	**−299**[c]

DONO combination overtones discussed above, spectroscopic features due to DNO$_3$ were observed around 6143 and 7608 cm^{-1}. Even though it is expected that DNO$_3$ is formed as a by-product of the heterogeneous reaction of D$_2$O and NO$_2$ (see Fig. 3), it was validated with a sample of pure DNO$_3$ that the bands centred at 6142.5 cm^{-1} and 7607.6 cm^{-1} can be assigned to bands of deuterated nitric acid. It is highly likely that the former represents the $2\nu_1 + \nu_3$ combination band of DNO$_3$, while the latter corresponds to the $3\nu_1$ overtone, as calculated from the mid-infrared bands of DNO$_3$ [37]. The respective spectral regions are shown in Fig. 6; the rotational structure of both bands is not fully resolved, but sharp Q-branches located at 6142.5 cm^{-1} and 7607.6 cm^{-1} dominate the bands in both cases, as previously observed for HNO$_3$ [17]. Note that *a*-type bands are expected for these overtone and combination vibrations involving ν_1 also in DNO$_3$.

4. Conclusions

In this study, the first observation of combination and overtone bands $2\nu_1 + \nu_3$ (6212.0 cm^{-1}) and $3\nu_1$ (7691.8 cm^{-1}) of *trans*-DONO and of the $3\nu_1$ (~7302.5 cm^{-1}) of *cis*-DONO in the near-infrared is reported. The spectra were recorded using FT-IBBCEAS and show the high suitability of this method for measurements of isotopic trace species. In addition, due to the formation of deuterated nitric acid in the same experiment, two new bands of DNO$_3$ at 6142.5 cm^{-1} and 7607.6 cm^{-1} were observed, which are very likely assigned to the $2\nu_1 + \nu_3$ and $3\nu_1$ respectively. Follow-up high resolution measurements of these isotopologues as well as high-end theoretical calculations of this interesting region are highly desirable.

CRediT authorship contribution statement

Ranjini Raghunandan: Investigation, Software, Formal analysis, Writing - original draft, Funding acquisition. **Johannes Orphal:** Formal analysis, Software, Validation, Writing - review & editing, Simulation, Resources. **Albert A. Ruth:** Conceptualization, Methodology, Writing - review & editing, Resources, Supervision, Project administration, Funding acquisition.

Declaration of Competing Interest

The authors declare that they have no known competing financial interests or personal relationships that could have appeared to influence the work reported in this paper.
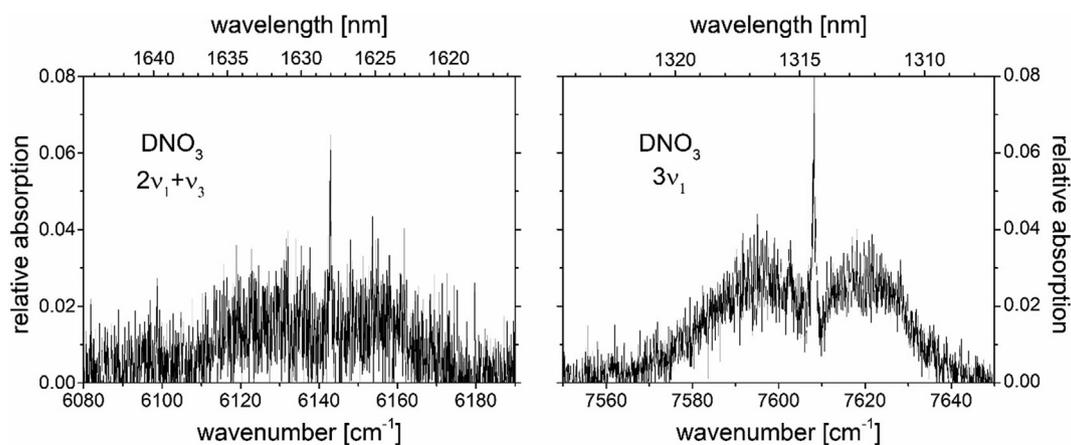
Acknowledgements

Fig. 6. Two near-infrared combination and overtone bands of deuterated nitric acid (DNO$_3$) centred at 6142.5 cm^{-1} (left panel) and 7607.6 cm^{-1} (right panel). The bands are most likely due to $2\nu_1$-+-ν_3 and $3\nu_1$ of DNO$_3$, respectively.

References

[1] J.M. Guilmot, M. Godefried, M. Herman, Rovibrational parameters for *trans*-nitrous acid, J. Mol. Spectrosc. 160 (1993) 387–400, https://doi.org/10.1006/jmsp.1993.1186.

[2] R.H. Kagann, A.G. Maki, Infrared absorption intensities of nitrous acid (HONO) fundamental bands, J. Quant. Spectrosc. Rad. Trans. 30 (1983) 37–44, https://doi.org/10.1016/0022-4073(83)90071-7.

[3] C.M. Deeley, M. Mills, The infrared vibration-rotation spectrum of trans and cis nitrous acid, J. Mol. Struture 100 (1983) 199–213, https://doi.org/10.1016/0022-2860(83)90092-3.

[4] A. Perrin, S. Miljanic, A. Dehayem-Kamadjeu, P. Chelin, J. Orphal, J. Demaison, The 14–22 μm absorption spectrum of nitrous acid studied by high-resolution Fourier-transform spectroscopy: new analysis of the ν_5 and ν_6 interacting bands of *trans*-HONO and first analysis of the ν_6 band of *cis*-HONO, J. Mol. Spectrosc. 245 (2007) 100–108, https://doi.org/10.1016/j.jms.2007.07.007.

[5] D. Yamano, A. Yabushita, M. Kawasaki, A. Perrin, Absorption spectrum of nitrous acid for the $\nu_1 + 2\nu_3$ band studied with continuous-wave cavity ring-down spectroscopy and theoretical calculations, J. Quant. Spectrosc. Rad. Trans. 111 (2010) 45–51, https://doi.org/10.1016/j.jqsrt.2009.07.009.

[6] V. Sironneau, J. Orphal, J. Demaison, P. Chelin, High-resolution infrared spectroscopy of *trans*- and *cis*-H^{18}ON^{18}O: equilibrium structures of the nitrous acid isomers, J. Phys. Chem. A 112 (2008) 10697–10702, https://doi.org/10.1021/jp806286p.

[7] I. Kleiner, J.M. Guilmot, M. Carleer, M. Herman, The ν_4 fundamental bands of *trans*- and *cis*-HNO$_2$, J. Mol. Spectrosc. 149 (1991) 341–347, https://doi.org/10.1016/0022-2852(91)90290-Q.

[8] A.G. Maki, R.L. Sams, Diode laser spectra of *cis*-HONO near 850 cm^{-1} and *trans*-HONO near 1700 cm^{-1}, J. Mol. Struct. 100 (1983) 215–221, https://doi.org/10.1016/0022-2860(83)90093-5.

[9] S.M. Holland, R.J. Stickland, M.N.R. Ashfold, D.A. Newnham, I.M. Mills, Vibrationally mediated photodissociation of nitrous acid, J. Chem. Soc., Faraday Trans. 87 (1991) 3461–3472, https://doi.org/10.1039/FT9918703461.

[10] D. Luckhaus, The vibrational spectrum of HONO: fully coupled 6D direct dynamics, J. Chem. Phys. 118 (2003) 8797–8806, https://doi.org/10.1063/1.1567713.

[11] C. Jain, P. Morajkar, C. Schoemaecker, B. Viskolcz, C. Fittschen, Measurement of absolute absorption cross sections for nitrous acid (HONO) in the near-infrared region by the continuous wave cavity ring-down spectroscopy (cw-CRDS) technique coupled to laser photolysis, J. Phys. Chem. A 115 (2011) 10720–10728, https://doi.org/10.1021/jp203001y.

[12] A. Dehayem-Kamadjeu, O. Pirali, J. Orphal, I. Kleiner, P.M. Flaud, The far-infrared rotational spectrum of nitrous acid (HONO) and its deuterated species (DONO) studied by high-resolution Fourier-transform spectroscopy, J. Mol. Spectrosc. 234 (2005) 182–189, https://doi.org/10.1016/j.jms.2005.09.006.

[13] L.O. Halonen, C.M. Deeley, I.M. Mills, V.-M. Horneman, Vibration–rotation spectra of deuterated nitrous acid, DONO, Can. J. Phys. 62 (1984) 1300–1305, https://doi.org/10.1139/p84-176.

[14] A. Dehayem-Kamadjeu, J. Orphal, N. Ibrahim, I. Kleiner, O. Bouba, P.-M. Flaud, The ν_1 fundamental bands of *trans*- and *cis*-DONO studied by high-resolution Fourier-transform spectroscopy, J. Mol. Spectrosc. 238 (2006) 29–35, https://doi.org/10.1016/j.jms.2006.04.005.

[15] B. Alicke, A. Geyer, A. Hofzumahaus, F. Holland, S. Konrad, H.W. Patz, OH formation by HONO photolysis during the BERLIOZ experiment, J. Geophys. Res. - Atmos. 108 (2003) 8247–8263, https://doi.org/10.1029/2001JD000579.

[16] R. Volkamer, P. Sheehy, L.T. Molina, M.J. Molina, Oxidative capacity of the Mexico City atmosphere – Part 1: A radical source perspective, Atmos. Chem. Phys. 10 (2010) 6969–6991, https://doi.org/10.5194/acp-10-6969-2010.

[17] K.J. Feierabend, D.K. Havey, M.E. Varner, J.F. Stanton, V. Vaida, A comparison of experimental and calculated spectra of HNO$_3$ in the near-infrared using Fourier transform infrared spectroscopy and vibrational perturbation theory, J. Chem. Phys. 124 (2006) 124323, https://doi.org/10.1063/1.2180248.

[18] K.A. Ramazan, D. Syomin, B.J. Finlayson-Pitts, The photochemical production of HONO during the heterogeneous hydrolysis of NO$_2$, PCCP 6 (2004) 3836–3843, https://doi.org/10.1039/b402195a.

[19] K.A. Ramazan, L.M. Wingen, Y. Miller, G.M. Chaban, R.B. Gerber, S.S. Xantheas, B.J. Finlayson-Pitts, New experimental and theoretical approach to the heterogeneous hydrolysis of NO$_2$: key role of molecular nitric acid and its complexes, J. Phys. Chem. A 110 (2006) 6886–6897, https://doi.org/10.1021/jp056426n.

[20] Y. Miller, G.M. Chaban, B.J. Finlayson-Pitts, R.B. Gerber, Photochemical processes induced by vibrational overtone excitations: dynamics simulations for *cis*-HONO, *trans*-HONO, HNO$_3$, and HNO$_3$-H$_2$O, J. Phys. Chem. A 110 (2006) 5342–5354, https://doi.org/10.1021/jp0559940.

[21] M. Djehiche, A. Tomas, C. Fittschen, P. Coddevill, First direct detection of HONO in the reaction of methylnitrite (CH$_3$ONO) with OH radicals, Environ. Sci. Technol. 45 (2011) 608–614, https://doi.org/10.1021/es103076e.

[22] L.H. Jones, R.M. Badger, G.E. Moore, The infrared spectrum and the structure of gaseous nitrous acid, J. Chem. Phys. 19 (1951) 1599–1604, https://doi.org/10.1063/1.1748129.

[23] G.E. McGraw, D.L. Bernitt, I.C. Hisatsune, Infrared spectra of isotopic nitrous acids, J. Chem. Phys. 45 (1966) 1392–1399, https://doi.org/10.1063/1.1727772.

[24] R. Varma, R.F. Curl, Study of the N$_2$O$_3$-H$_2$O-HNO$_2$ equilibrium by intensity measurements in microwave spectroscopy, J. Phys. Chem. 80 (1976) 402–409, https://doi.org/10.1021/j100545a013.

[25] V. Sironneau, J.-M. Flaud, J. Orphal, I. Kleiner, P. Chelin, Absolute line intensities of HONO and DONO in the far-infrared and re-determination of the energy difference between the trans- and cis-species of nitrous acid, J. Mol. Spectrosc. 259 (2004) 100–104, https://doi.org/10.1016/j.jms.2009.11.013.

[26] F. Richter, M. Hochlaf, P. Rosmus, F. Gatti, H.-D. Meyer, A study of the mode selective trans-cis isomerization in HONO using ab initio methodology, J. Chem. Phys. 120 (2004) 1306–1317, https://doi.org/10.1063/1.1632471.

[27] J. Orphal, A.A. Ruth, High-resolution Fourier-transform cavity-enhanced absorption spectroscopy in the near-infrared using an incoherent broad-band light source, Opt. Express 16 (2008) 19232–19243, https://doi.org/10.1364/OE.16.019232.

[28] A.A. Ruth, J. Orphal, S.E. Fiedler, Cavity enhanced Fourier transform absorption spectroscopy using an incoherent broadband light source, Appl. Opt. 46 (2007) 3611–3616, https://doi.org/10.1364/AO.46.003611.

[29] S.E. Fiedler, A. Hese, A.A. Ruth, Incoherent broadband cavity enhanced absorption spectroscopy, Chem. Phys. Lett. 371 (2003) 284–294, https://doi.org/10.1016/S0009-2614(03)00263-X.

[30] A.A. Ruth, S. Dixneuf, R. Raghunandan, Cavity enhanced spectroscopy and sensing, in: G. Gagliardi, H.P. Loock (Eds.), 179 Springer Series in Optical Sciences, 2014, pp. 485–517, , https://doi.org/10.1007/978-3-642-40003-2.

[31] D.M. O'Leary, A.A. Ruth, S. Dixneuf, J. Orphal, R. Varma, The near infrared cavity-enhanced absorption spectrum of methylcyanide, J. Quant. Spectr. Rad. Trans. 113 (2012) 1138–1147, https://doi.org/10.1016/j.jqsrt.2012.02.022.

[32] R. Raghunandan, A. Perrin, A.A. Ruth, J. Orphal, First analysis of the $2\nu_1 + 3\nu_3$ band of NO$_2$ around 7192 cm^1, J. Mol. Spectrosc. 297 (2014) 4–10, https://doi.org/10.1016/j.jms.2013.12.007.

[33] J.K.G. Watson, Simplification of the molecular vibration-rotation Hamiltonian, Mol. Phys. 15 (1968) 479–490, https://doi.org/10.1080/00268976800101381.

[34] C.M. Western, PGOPHER, A program for simulating rotational, vibrational and electronic spectra, J. Quant. Spectrosc. Rad. Transfer 186 (2016) 221–242, https://doi.org/10.1016/j.jqsrt.2016.04.010.

[35] V.P. Bulychev, M.V. Buturlimova, K.G. Tokhadze, Anharmonic calculation of structural and spectroscopic parameters of the *cis*-DONO molecule, J. Phys. Chem. A 119 (2015) 9910–9916, https://doi.org/10.1021/acs.jpca.5b06466.

[36] F. Mélen, M. Herman, Vibrational bands of H$_x$N$_y$O$_z$ molecules, J. Phys. Chem. Ref. Data 21 (1992) 831–881, https://doi.org/10.1063/1.555916.

[37] G.E. McGraw, D.L. Bernitt, I.C. Hisatsune, Vibrational spectra of isotopic nitric acids, J. Chem. Phys. 42 (1965) 237–244, https://doi.org/10.1063/1.1695682.